Published in final edited form as:
Neurobiol Aging. 2012 April ; 33(4): 670–680. doi:10.1016/j.neurobiolaging.2010.06.003.

Homocysteine, neural atrophy, and the effect of caloric restriction in rhesus monkeys

AA Willette[b,c,d], **C Gallagher**[a,e], **BB Bendlin**[a,c,f], **DG McLaren**[a,c,g], **EK Kastman**[a,c], **E Canu**[a], **KJ Kosmatka**[a,c], **AS Field**[h], **AL Alexander**[d], **RJ Colman**[i], **ML Voytko**[j], **RH Weindruch**[f,i], **CL Coe**[b,d], and **SC Johnson**[*,a,c,f,g,i]

[a]Geriatric Research Education and Clinical Center, Wm. S. Middleton Memorial Veterans Hospital, Madison, WI 53705, USA

[b]Harlow Primate Laboratory, Department of Psychology, University of Wisconsin-Madison, Madison, WI 53715, USA

[c]Wisconsin Alzheimer's Disease Research Center, University of Wisconsin School of Medicine and Public Health, Madison, WI, 53705 USA

[d]Waisman Laboratory for Brain Imaging and Behavior, University of Wisconsin-Madison, 13 Madison, WI, 53705

[e]Department of Neurology, University of Wisconsin-Madison, Madison, WI 53792 USA

[f]Department of Medicine, University of Wisconsin, Madison, WI, 53705 USA

[g]Neuroscience Training Program, University of Wisconsin, Madison, WI 53706. USA

[h]Department of Radiology, University of Wisconsin, Madison, WI, 53792 USA

[i]Wisconsin National Primate Research Center, Madison, WI, 53715 USA

[j]Department of Neurobiology & Anatomy, School of Medicine, Wake Forest University, Winston-Salem, NC 27157 USA

Abstract

Higher serum homocysteine (Hcy) levels in humans are associated with vascular pathology and greater risk for dementia, as well as lower global and regional volumes in frontal lobe and hippocampus. Calorie restriction (CR) in rhesus monkeys (*Macaca mulatta*) may confer neural protection against age- or Hcy-related vascular pathology. Hcy was collected proximal to an MRI acquisition in aged rhesus monkeys and regressed against volumetric and diffusion tensor imaging indices using voxel-wise analyses. Higher Hcy was associated with lower white matter volume in pons and corpus callosum. Hcy was correlated with lower gray matter volume and density in prefrontal cortices and striatum. CR did not influence Hcy levels. However, control monkeys exhibited a strong negative correlation between Hcy and global gray matter, whereas no relationship was evident for the CR monkeys. Similar group differences were also seen across modalities in the splenium of the corpus callosum, prefrontal cortices, hippocampus, and

[*]**Send Correspondence to**: Sterling C. Johnson, Geriatric Research Education and Clinical Center, D-4225 Veterans Administration Hospital, 2500 Overlook Terrace, Madison, WI 53705, USA, Phone: (608) 256-1901, scj@medicine.wisc.edu .

Disclosure Statement

The authors have no actual or perceived conflicts of interest regarding the content of this manuscript.

somatosensory areas. The data suggest that CR may ameliorate the influence of Hcy on several important age-related parameters of parenchymal health.

Keywords

rhesus monkey; aging; homocysteine; neural atrophy; voxel-based morphometry; diffusion tensor imaging; caloric restriction; primate

1. Introduction

Homocysteine (Hcy), biosynthesized from the essential amino acid methionine, is associated with pathological aging and is a candidate biomarker of cardiovascular and dementia risk (McCully, 2001; Blasko et al., 2008; Zylberstein et al., 2009). Circulating levels of Hcy in humans tend to increase with age and contribute to cerebrovascular pathology in part through endothelial thrombosis, fibrous arteriosclerotic plaques, and degradation of the epithelial cells in the blood vessel wall (Marlatt et al., 2008). Higher circulating Hcy has been associated with smaller total brain volume (Seshadri et al., 2008), lower regional volumes including hippocampus (den Heijer et al., 2003; Wilhelm et al., 2008), and perhaps by extension cognitive decline (Nurk et al., 2005).

In rats, infusion of Hcy via microdialysis into the striatum resulted in hypersecretion of excitatory amino acids and more brain damage following experimentally induced strokes (Ganguly et al., 2008). In addition, serum Hcy has been correlated with hippocampal degeneration related to alcohol dependence (Wilhelm et al., 2008), as well as with lower temporal and frontal lobar volumes (Seshadri et al., 2008). Hcy also may sensitize dopaminergic neurons to environmental toxins and adversely hamper DNA repair (Margas et al., 2004). Higher levels of Hcy are also detected in the cerebellum across a wide variety of species relative to whole brain (Broch and Ueland, 1984). Oligodendrocytes appear to be especially sensitive to Hcy-related damage, as Hcy is highly associated with axonal demyelination as well as periventricular and subcortical white matter hyperintensities (Vermeer et al., 2002; Wong et al., 2006). However, Hcy does not appear to adversely impact all brain structures such as the amygdala (den Heijer et al., 2003), and others have found no relationship between Hcy levels and central white and gray matter volumes (Longstreth et al., 2004; Morra et al., 2009).

We sought to extend and clarify these findings in an established non-human primate model of aging, the rhesus monkey, which shows many similar physiological and neural changes to humans during aging (Roth et al., 2004). Although Hcy levels do not appear to rise as markedly with age in non-human primates (Preston et al., 2002), dietary manipulations that result in transient hyperhomocysteinemia do impact vasculature physiology in the expected atherogenic manner (Harker et al., 1976; Lentz et al., 1996, 2001).

Our cohort of monkeys was derived from a longitudinal study on the benefits of consuming a calorie restriction diet (CR; Colman et al., 2009). In addition to a salubrious change in glucoregulation, CR confers protective effects on the vasculature in this specific sample and rhesus monkeys in general--despite the fact that cardiovascular disease rarely occurs in this species unless experimentally placed on a high fat diet (Edwards et al., 1998; Ungvari et al., 2008). By extension, CR may still reduce Hcy concentrations and/or protect against Hcy-associated changes in the aging brain. Rhesus monkeys do not show an overall decrease in brain weight in old age (Herndon et al., 1998), but do evince reductions in gray matter and white matter in many regions (Wisco et al., 2008).

Because aging is related to lower regional volume in diffuse areas (Sowell et al., 2003), a previously validated voxel-wise approach (McLaren et al., 2009) was used to gauge the association of Hcy with both global and regional white matter and gray matter volumes. In addition, the microstructural tissue density of myelin and axons was determined via diffusion tensor imaging and estimated by fractional anisotropy, followed by axial diffusivity (λ_1) and radial diffusivity ($[\lambda_2 + \lambda_3] / 2$]), in order to examine whether fractional anisotropy changes were related primarily to alterations in axons or myelin (Song et al., 2002). Tissue density of gray matter and white matter was also jointly determined using mean diffusivity. Finally, we investigated if monkeys on the CR diet showed less Hcy related atrophy relative to control animals per unit increase in Hcy (μmol/L). These analyses were conducted using cross-sectional MRI and physiological data.

2. Subjects and methods

2.1. Study population

Forty-five rhesus monkeys (*Macaca mulatta*) between 19 and 31 years of age were used from a larger longitudinal CR project at the Wisconsin National Primate Research Center. 18 animals were fed a normative diet of commercial chow (mean age ± SD, 23.84 ± 2.79; 12 females, 6 males), while 27 CR subjects (mean age ± SD, 24.32 ± 2.77; 15 females, 12 males) had been on a moderately restricted diet (30% reduction of intake) for approximately 12 to 17 years starting in 1989. Details of the CR manipulation have been described previously (Kemnitz et al., 1993; Ramsey et al., 2000). Animal rooms were maintained at 21 °C on a 12h/12h light-dark cycle. Water was available *ad libitum*. Food was present for 6-8 h per day. Monkeys were individually housed, remained in their home cage except during assessments, and were monitored at least twice daily by care and research staff. The study was approved by the Institutional Animal Care and Use Committee. Investigators processing and analyzing imaging or serum data were blind to dietary condition.

2.2 Data collection

The single MRI scan session and image acquisition parameters have been described previously (Colman et al., 2009; Bendlin et al., in press). Briefly, animals were maintained in an optimal plane of anesthesia while images were acquired using a General Electric 3.0 T scanner (GE Medical Systems, Milwaukee, WI, USA). T1- and T2-weighted scans were used to determine global and regional gray matter and white matter volumes. Diffusion tensor imaging was used to quantitatively estimate microstructural density of gray matter and white matter tissue density (Song et al., 2002; Hasan et al., 2008). Blood was collected within 6 months preceding the MRI scan to quantify circulating Hcy levels.

2.3. Hcy measurement

Fasted whole blood was collected via femoral or saphenous venipuncture from conscious animals while briefly restrained, allowed to clot for up to 30 minutes, and then centrifuged to derive serum (Willette et al., 2007). An Enzyme Immunoassay kit designed for detection of human Hcy was used to determine levels of unbound L-Hcy as described by the manufacturer (Axis-Shield Diagnostics Ltd., Dundee, United Kingdom). Because crossreactivity with the monkey samples was unknown, several specimens from aged humans were included in the assay to verify its reliability, appropriateness, and accuracy of the standard reference curve. The kit range was 1-30 μmol/L.

2.4. Non-MRI statistical analyses

Independent samples t-tests or Analysis of Variance (ANOVA) in SPSS 16.0 (SPSS, Chicago) was used to assess group differences for demographic variables, Hcy, and global

brain volumes, as well as interactions. Distribution plots and skewness of the variables were computed to confirm the appropriateness of using them in a General Linear Model for voxel-wise analyses. Two-tailed Pearson's r correlations examined associations between a given dependent variable and Hcy, and whether these relationships were modified by dietary condition.

2.5. Imaging artifacts

Images were inspected by a neuroradiologist (ASF) in order to locate scan artifacts that could influence regional volumetric or microstructural results. One T1-weighted and three diffusion tensor imaging scans had motion, respiratory, phase, or other artifacts that rendered data unusable for regional brain analyses and were excluded. Six diffusion tensor imaging scans (Controls = 2, CR = 4) had punctate (~1-2 mm) abnormalities located in the white matter of the dorsal convexity that were proximal to primary motor and somatosensory areas. These scans were also not analyzed because such abnormalities can bias voxel-wise analyses and create spurious results. The nature of these abnormalities will be investigated in a future histology report.

2.6. MRI processing

T1-weighted images were segmented and normalized to 112RM-SL atlas space using DARTEL (Ashburner; 2007; McLaren et al., 2009, 2010). In order to optimize signal to noise and facilitate comparison across participants, gray matter and white matter segments were smoothed using a 4mm full width half maximum Gaussian kernel. Gray matter and white matter volumes were masked using binary transforms of prior probability maps. Fractional anisotropy, mean diffusivity, axial diffusivity, and radial diffusivity maps were computed from diffusion tensor imaging data using DTIFIT in FSL (http://www.fmrib.ox.ac.uk/fsl/fdt/fdt_dtifit.html). Diffusion tensor imaging measurements were aligned to the 112RM-SL atlas space with the following procedure: each individual's B0 image was normalized to a T2-weighted atlas template (McLaren et al. 2009), along with the normalization parameters to the diffusion tensor imaging measurements. The normalized images were then smoothed with a 4mm full width half maximum Gaussian kernel. Fractional anisotropy analyses were masked using a binary white matter mask to restrict the analysis to major fiber tracts. Because variations in volume can affect estimates of tissue density, an absolute threshold of 0.1 was applied to fractional anisotropy maps to reduce the influence of white matter morphology on results. Mean diffusivity maps were masked using a binary version of the 112RM-SL rhesus brain, because mean diffusivity is not biased toward gray matter or white matter tissue classes relative to fractional anisotropy. Mean diffusivity results did not change when binary gray matter and white matter prior probability maps were separately used as masks and the resulting mean diffusivity maps combined. Region of interest drawing of the hippocampus was conducted by an expert (AAW) for the purpose of better specifying Monte Carlo simulations and voxel-wise analysis of that structure (see below).

2.7. MRI analyses

Multiple regression voxel-wise analyses were conducted in SPM5 (http://www.fil.ion.ucl.ac.uk/spm/software/spm5/) using a general linear model (Ashburner and Friston, 2000). Hcy was the independent variable and age, gender, and condition (CR versus control) were covariates; total brain volume (global gray matter + global white matter) was additionally included in volumetric analyses. Volumetric or diffusion tensor imaging maps were used as dependent variables in separate models. In addition, we added an Hcy*Condition interaction term to the existing models for each modality, to separately evaluate whether CR modified the regional associations of Hcy relative to controls. The t-statistic threshold was set at $p < 0.005$ (uncorrected). These analyses were corrected for

multiple comparisons at the cluster level using Monte Carlo simulations with an alpha of .05 (Forman et al., 1995). The reference guide on AFNI's website was used (http://afni.nimh.nih.gov/pub/dist/doc/manual/AlphaSim.pdf). This iterative permutation technique estimates the probability of generating a cluster with n voxels based on randomly generated images with the same dimensions, voxel probability threshold, and smoothing parameters as MRI images inputted for analysis. Although violation of non-stationarity is a concern for cluster correction of imaging data, the use of a 4 mm full width half maximum kernel does not appreciably bias the true alpha when using this permutational estimate of cluster size (Hayasaka et al., 2004). For gray matter volumes, cluster correction required 884 voxels or more to reach significance. White matter volume and fractional anisotropy specific to white matter needed at least 868 voxels within a cluster. Mean diffusivity clusters within gray matter and white matter were significant only if they were larger than 1,075 voxels. Finally, a simulation was conducted within a bilateral ROI of hippocampus and yielded a corrected cluster size at or above 164 voxels that would be significant for that structure.

Whole brain cluster coordinates correspond to the space of the Saleem-Logothetis atlas (Saleem et al., 2002) and are displayed on the 112RM-SL underlays (McLaren et al., 2009). To investigate if differences in myelin or axons predominantly drove regional fractional anisotropy results (Song et al., 2002), a binary transform of the Hcy fractional anisotropy association map was used as an explicit mask for post-hoc voxel-wise analyses of radial and axial diffusivity with a voxel threshold of $p < .05$ (uncorrected) in at least 50 contiguous voxels. Major fiber tracts were identified based on an autoradiography atlas of rhesus monkey brains (Schmahmann and Pandya, 2006). Sub-cortical rhombencephalon, mesencephalon, and diencephalon structures were determined using the rhesus monkey atlas of Paxinos and co-workers (2009).

3. Results

3.1. Hcy and demographics

The dietary groups did not differ significantly by age or gender. Hcy values for the monkeys were within the standard reference curve of the assay kit, comparable to human values, and conformed to a Gaussian distribution without significant skewness. One CR animal had an Hcy value (25 μmol/L) more than three standard deviations above the sample mean and was excluded from analyses. The presence or absence of this animal's data did not affect the physiological or neural results beyond a loss of power. The range of Hcy was 4.54-20.32 μmol/L (mean = 8.87; SD = 3.93), and the average levels for the CR monkeys did not differ significantly from the control animals (9.33 ± .84 vs. 8.16 ± .80, respectively). The elapsed time interval between the blood collection and date of the MRI scan was no correlated with Hcy levels or associations with neural indices.

3.2. Hcy and global volumes

Total brain volume did not differ between groups. Higher Hcy levels were associated with lower global white matter [$r(44) = -.315$, $p < .05$], while no relationship was found with global gray matter or total brain volume. However, there was a significant Hcy*Condition interaction for global gray matter volume [$F(1,40)=6.38$, $p < .05$]. Post-hoc split level correlations revealed a negative relationship between Hcy and global gray matter volume among controls [$r(18) = -0.61$, $p < .01$], but a non-significant relationship for CR animals [$r(26) = 0.16$, $p = .44$]. All subsequent interaction analyses, therefore, tested only the question of whether or not a CR diet conferred an ameliorative effect on the association between Hcy and the brain indices on a regional voxel-wise basis.

3.3. Hcy and regional volumetric analyses

3.3.1. White matter: associations—Higher Hcy levels were associated with lower white matter volume throughout the pons (Figure 1; Table 1). Part of the cluster ascended into the middle cerebellar penducle and included pontocerebellar fibers, extending along ventral paraflocculus and lobules 2-5 into anterior cerebellum. Portions of this cluster also ascended through the inferior cerebellar peduncle into lobules 1-4, deep white matter of lateral posterior cerebellar hemispheres, and deep structures, including the basal interstitial, interposed, medial, lateral, and floccular nuclei. A separate cluster incorporated the body of the corpus callosum; coverage extended to thalamic white matter bundles in both hemispheres subjacent to the head of the caudate, as well as in the pontine bundle.

3.3.2. White matter: dietary condition*Hcy interaction—No clusters related to white matter exceeded the statistical threshold after correction.

3.3.3. Gray matter: associations—Higher Hcy levels were correlated with smaller gray matter volume maximally in the medial inferior branch of cingulate sulcus, including the mid- and anterior cingulate cortices; the anterior-posterior extent was approximately 17 mm (Figure 2B-C; Table 2). A cluster of interest was also detected bilaterally in the caudate and putamen (Figure 2A), extending to orbital prefrontal cortex rostrally and laterally into the agranular insula area. A region encompassing dorsal premotor and dorsal prefrontal cortices was also associated with Hcy.

3.3.4. Gray matter: Hcy*dietary condition interaction—This interaction model tested if CR monkeys, per μmol/L unit increase in basal Hcy, showed a smaller or non-significant relationship between Hcy and gray matter volume when compared to control animals. In the maxima within somatosensory areas 1 and 2 (Figure 2E; Table 2), animals on control diets showed a strong negative correlation between Hcy and gray matter volume in left parietal lobe [$r(17) = -.61$, $p = .009$] (Figure 2F), which was similar to the global gray matter association. By contrast, higher Hcy levels among CR monkeys were non-significantly related to more gray matter [$r(26) = .37$, $p = .062$]. This reduction of the association with Hcy in CR monkeys was also found in right somatosensory areas 1 and 2, 3a/b, and 5, as well as visual area 7a of parietal cortex, right hippocampus, and left visual cortices (Figure 2E).

3.4. Hcy and microstructural indices

3.4.1. Fractional anisotropy, radial diffusion, and axial diffusion: associations —Hcy levels were also correlated with lower fractional anisotropy maximally in cerebellar white matter immediately dorsal to the fourth ventricle bilaterally (Figure 3A; Table 3). This cluster was similar to the white matter volume results. Associated fibers in this region include the superior cerebellar peduncles, as well as midbrain around the dorsal raphe and occulomotor nuclei (Figure 3B). Follow-up voxel-wise post hoc analyses of radial and axial diffusivity were performed using a binary transform of the fractional anisotropy result map as an explicit mask. The radial diffusivity map revealed the same clusters and degree of significance as the fractional anisotropy map, such as ponto-cerebellar fibers of the middle cerebellar peduncle ($x = -2$, $y = -1$, $z = 8$; cluster size = 791; $t = 4.29$), whereas the axial diffusivity map showed only one small cluster in anterior cerebellum also near the peduncle ($x = 0$, $y = -2$, $z = 9$; cluster size = 121; $t = 3.62$).

3.4.2. Fractional anisotropy: Hcy*dietary condition interaction—An Hcy*Condition interaction was added to the association model to test whether or not the association between white matter density and Hcy levels differed between groups. As found in previous analyses, per μmol/L unit increase of Hcy, the association was reduced in CR

animals relative to monkeys consuming control diets. The global maximum after correction was located within dorsal occipital bundle lateral to extrastriate cortex and extended through the splenium (Figure 3E-F; Table 3). Among the controls, Hcy levels were correlated with lower fractional anisotropy [$r(18) = -.61$, $p = .005$], while the relationship in CR monkeys did not reach statistical significance [$r(17) = .39$, $p = .120$] (Figure 3G).

3.4.3. Mean diffusivity: associations—Higher Hcy concentrations were maximally related to lower tissue density within a bilateral cluster in anterior cerebellum along lobules 3-4 (Figure 3B; Table 4). This region included fibers ascending through the superior cerebellar peduncle akin to the fractional anisotropy analysis, ending in the periaqueductal gray ventral to inferior colliculus. A prefrontal region encapsulated ventral prefrontal cortex and central orbital prefrontal cortex (area 11L), as well as dorsal prefrontal cortex adjacent the principle sulcus (Figure 3C-D). For white matter microstructure, rostral fibers included corticocortical prefrontal cortex connections and extreme capsule.

3.4.4. Mean diffusivity: Hcy*dietary condition interaction—A Hcy*Condition model tested if CR monkeys had lower mean diffusivity relative to controls per μmol/L increase in Hcy. The specific hypothesis was that the CR diet would reduce the relationship between Hcy and tissue density. The global maximum was located bilaterally in dorsal prefrontal cortex, extending into frontal pole, medial prefrontal cortex along the frontal forceps, and caudally in to anterior cingulate cortex (Figure 3E-F; Table 4). A smaller area in primary visual cortex was also apparent. A split level correlation of a voxel in this region indicated the expected positive relationship of lower Hcy with higher mean diffusivity among controls [$r(18) = .69$, $p = .001$], but no significant relationship among CR monkeys [$r(17) = -.44$, $p = .075$] (Figure 3H).

4. Discussion

Serum Hcy was detected at levels within the range of reference human values in 45 aged rhesus monkeys, and was related to altered volumetric and microstructural tissue density indices in prefrontal, parietal, temporal, and subcortical areas previously found to be sensitive to presumed cerebrovascular changes. Hcy was non-significantly higher in our CR animals. A similar CR manipulation lasting 3 months also found a non-significant 6.43% increase in Hcy (Chen et al., 2009).

Despite statistically comparable Hcy concentrations in the CR and control groups, the association between higher Hcy levels and lower global gray matter volume in the control group was not observed in CR animals. These results suggest that CR may potect the brain against the adverse affects of Hcy, or from effects of aging for which Hcy is a biomarker. Because CR downregulates arterial proteoglycans and shrinks low density lipoprotein size in this cohort of monkeys (Edwards et al., 1998), these animals may have been protected against damage to the vascular endothelium and consequent regional neuronal ischemia that could affect brain tissue volumes. For example, CR may have an effect on basal nitric oxide levels because it is associated with endothelial health. Mice on a 35% CR diet following hindlimb ischemic surgery show increased nitric oxide synthase phosphorylation of endothelial cells (Kondo et al., 2009), which could counteract Hcy induced decreases in nitric oxide that render microvascular lumen less distensible. Alternatively, CR could cause Hcy to be more efficiently converted into cysteine through either: 1) increased expression of the catalyzing agents Cystathionine β-synthase or Cystathionine β-lyase; or 2) higher concentrations of pyroxidine (vitamin B_6). Twenty-four hour fasting among rats raised cysteine levels compared to *ad libitum* feeding in the same subjects, although the effect was non-significant (Smolin and Benevenga, 1984).

With respect to regional gray matter volume, higher Hcy levels were related to a global maximum in a bilateral cluster encompassing anterior cingulate cortex. In the Framingham Offspring study, total Hcy levels were inversely related to frontal lobe volume (Seshadri et al., 2008), and a voxel-based morphometry assessment of B vitamin supplementation specifically implicated a similar location in humans (Erickson et al., 2008). Most additional anatomic regions identified in the latter study corresponded to our regional gray matter findings in monkeys. These clusters included parietal cortex and intraparietal areas, cingulate cortex, supplementary motor area, and the cingulate sulcus. Furthermore, an ROI analysis associated higher Hcy with lower right hippocampus volume in alcoholic patients (Wilhelm et al., 2008). Ganguly and colleagues (2008) also found that microdialysis infusion of Hcy in anaesthetized rats exacerbated post-stroke damage to the striatum. Peripheral Hcy was related to less gray matter volume in both of these structures in our sample.

For our diffusion tensor imaging measures, the relationship between Hcy and gray matter tissue density as estimated by mean diffusivity was similar to the volumetric results in dorsal premotor and anterior cingulate cortices, as well as in the orbital prefrontal cortex and paralimbic structures, most of which can be affected by age or non-age related pathologies that raise Hcy (Thomas et al., 2002; Sowell et al., 2003; Shirpoor et al., 2009). It is possible that some cerebrovascular pathology may directly contribute to the structural changes in some of these regions. In addition, several rodent models show that application of Hcy causes direct neurotoxic effects on cerebellar purkinje and granule cells *in vitro* (Kim and Pae, 1996; Oldreive and Doherty, 2007).

Higher Hcy levels were associated with lower white matter volume and reduced fractional anisotropy in regions of efferent and afferent ponto-cerebellar connections and basis pontis. Higher radial diffusivity in the middle cerebellar peduncle and almost all other regions of altered fractional anisotropy suggested that these changes were more likely related to less myelin rather than fewer axons (Song et al., 2002). Hcy-related changes in white matter volume, unlike gray matter, were not modified by CR, although focal protection was evident in cortical and sub-cortical areas. A few neurological syndromes demonstrate selective vulnerability of the pons, cerebellar peduncles, and splenium to cerebrovascular injury. The pons and posterior white matter are specifically prone to damage during osmotic stress or hypertensive crisis (Pearce, 2009). Age-related cerebrovascular changes in the central pons ("pontine rarefaction") has been associated with symptoms of disequilibrium in elders and attributed to the effects of cerebrovascular disease on penetrating pontine arterioles (Pullicino et al., 1995; Kwa et al., 1998). Hcy also appears to be a useful biomarker for periventricular and deep white matter hyperintensities in normal aging, as well as in neurodegenerative disorders (Sachdev, 2004, 2005).

The pons and cerebellum have not typically been examined in these previous reports, but both were related to Hcy in our analyses. B_{12} deficiency, which results in elevated serum Hcy levels, can cause selective demyelination of the posterior columns of spinal cord, with similar abnormalities in the pons and cerebellar peduncles (Katsaros eta al., 1998). More diffuse leukoencephalopathy, also with occipital/parietal predominance, has been described in a case of uncontrolled homocystinuria (Vatanavicharn et al., 2008). Folate depletion versus repletion among murine dams raised Hcy levels and induced substantial cell reductions in pons and cerebellum of offspring (Xiao et al., 2005). Higher levels of Hcy may be implicated in degrading coursing fibers of the cerebellothalamocortical or corticopontocerebellar tracts. Indeed, the premotor cortices, the body of the corpus callosum, mid cingulate, and thalamic bundles all showed lower fractional anisotropy as Hcy concentrations increased. Patients with multiple sclerosis manifest lower fractional anisotropy and higher mean diffusivity in the body of the corpus callosum, displaying

dysregulation of activity in the above regions that grade for motor output (Lenzi et al., 2007). More broadly, lower fractional anisotropy in the prefrontal cortices, the genu of the corpus callosum, and other regions appear to be associated with a variety of behavioral deficits including reduced motor speed, executive functioning, and working memory (Kennedy and Raz, 2009).

Although hyperhomocysteinemia may directly induce the above effects, Hcy could alternatively serve as a risk marker rather than a true causal factor in its relationship to neural atrophy. Hcy can cause excitotoxicity by inducing oxidative stress, but it also sensitizes neurons to exogenous or endogenous toxins such as amyloid beta accumulation (Doherty, 2007). Higher Hcy also potentiates proinflammatory cytokine expression, which can dysregulate intracellular energy homeostasis (Karalis et al., 2009) and cause oxidative stress in a paracrine manner (Gokkusu et al., 2010). CR has been shown to reduce levels of these proteins in this monkey cohort (Willette et al., 2010) and non-obese adults on 20% CR diets (Fontana et al., 2007). While interleukin-6 levels did not mediate Hcy-related associations with neural regions in this sample (data not shown), CR may affect other inflammatory agents or similar factors that are potentiated by Hcy.

There are several limitations to the current study. Our MRI and physiological data were cross-sectional in nature and do not allow causal inferences to be made. Although we removed diffusion tensor imaging scans with artifacts in order to minimize the possibility of spurious results in voxel-wise analyses, this step could have inadvertently introduced selection bias in the interaction analyses for fractional anisotropy and mean diffusivity. We also did not collect gait or balance motor measures, which would have been a useful to regress onto the white matter volume map overlaying the pons and anterior cerebellum; future studies should examine this relationship.

In conclusion, this cross-sectional regression analysis of the associations among Hcy levels, gray matter and white matter volume, and microstructural density of parenchyma in rhesus monkeys confirms and extends previous ROI and lobar volume studies in humans. CR may provide protection from Hcy-related alterations in gray matter within prefrontal, parietal, and cerebellar regions. In contrast, CR did not appear to similarly lessen the impact of Hcy on white matter volume, although it did influence microstructural density of pontocerebellar fibers, corpus callosum, and other important tracts. CR may mitigate the Hcy-related volume loss in brain regions implicated in the development of movement, gait, and somatosensory difficulties with aging.

Acknowledgments

This study was supported in part by the National Institutes of Health RR000167, AG11915, AG000213, and GM007507. AAW was supported by the Ford Foundation, National Science Foundation, and a fellowship established by the Marian S. Schwartz fund. The study was also supported with resources and use of facilities at the William S. Middleton Memorial Veterans Hospital, Madison, WI, USA. The assistance of Brent W. Thiel, Michele E. Fitzgerald, Ron Fisher, Scott T. Baum, Josh Smith, Ricki J. Colman, Ph.D., Andy. A. Alexander, Ph.D., and the Waisman Center for Brain Imaging are greatly appreciated. GRECC Manuscript Number XXXX.

References

Ashburner J. A fast diffeomorphic image registration algorithm. Neuroimage. 2007; 38(1):95–113. [PubMed: 17761438]

Ashburner J, Friston KJ. Voxel-based morphometry--the methods. Neuroimage. 2000; 11(6 Pt 1):805–21. [PubMed: 10860804]

Bendlin BB, Canu E, Willette AA, Kastman EK, McLaren DG, Kosmatka KJ, Xu G, Field AS, Colman RJ, Coe CL, Weindruch RH, Alexander AL, Johnson SC. Effects of aging and calorie restriction on white matter in rhesus macaques. Neurobiology of Aging. In press.

Blasko I, Jellinger K, Kemmler G, Krampla W, Jungwirth S, Wichart I, Tragl KH, Fischer P. Conversion from cognitive health to mild cognitive impairment and Alzheimer's disease: Prediction by plasma amyloid beta 42, medial temporal lobe atrophy and homocysteine. Neurobiol Aging. 2008; 29(1):1–11. [PubMed: 17055615]

Broch OJ, Ueland PM. Regional distribution of homocysteine in the mammalian brain. J Neurochem. 1984; 43(6):1755–7. [PubMed: 6491675]

Chen FY, Chen SM, Huang HT, Lee SR, Liu YL, Jou HJ. Effects of a lifestyle program on risks for cardiovascular disease in women. Taiwan J Obstet Gynecol. 2009; 48(1):49–52. [PubMed: 19346192]

Colman RJ, Anderson RM, Johnson SC, Kastman EK, Kosmatka KJ, Beasley TM, Allison DB, Cruzen C, Simmons HA, Kemnitz JW, Weindruch R. Caloric restriction delays disease onset and mortality in rhesus monkeys. Science. 2009; 325(5937):201–4. [PubMed: 19590001]

Den Heijer T, Vermeer SE, Clarke R, Oudkerk M, Koudstaal PJ, Hofman A, Breteler MMB. Homocysteine and brain atrophy on MRI of non-demented elderly. Brain. 2002; 126(1):170–5. [PubMed: 12477704]

Doherty GH. Homocysteine: more than just a matter of life and death. Exp Neurol. 2007; 205(1):5–8. [PubMed: 17383638]

Edwards IJ, Rudel LL, Terry JG, Kemnitz JW, Weindruch R, Cefalu WT. Caloric restriction in rhesus monkeys reduces low density lipoprotein interaction with arterial proteoglycans. J Gerontol A Biol Sci Med Sci. 1998; 53(6):B443–8. [PubMed: 9823741]

Erickson KI, Suever BL, Prakash RS, Colcombe SJ, McAuley E, Kramer AF. Greater intake of vitamins B6 and B12 spares gray matter in healthy elderly: a voxel-based morphometry study. Brain Res. 2008; 1199:20–6. [PubMed: 18281020]

Forman SD, Cohen JD, Fitzgerald M, Eddy WF, Mintun MA, Noll DC. Improved assessment of significant activation in functional magnetic resonance imaging (fMRI): use of a cluster-size threshold. Magn Reson Med. 1995; 33(5):636–47. [PubMed: 7596267]

Ganguly PK, Maddaford TG, Edel AL, O K, Smeda JS, Pierce GN. Increased homocysteine-induced release of excitatory amino acids in the striatum of spontaneously hypertensive stroke-prone rats. Brain Res. 2008; 1226:192–8. [PubMed: 18598678]

Gokkusu C, Tulubas F, Unlucerci Y, Ozkok E, Umman B, Aydin M. Homocysteine and pro-inflammatory cytokine concentrations in acute heart disease. Cytokine. 50(1):15–8. [PubMed: 20129796]

Harker LA, Ross R, Slichter SJ, Scott RC. Homocysteine-induced artherosclerosis: Role of endothelial cell injury and platelet response to its genesis. J Clin Invest. 1976; 58:731–41. [PubMed: 821969]

Hasan KM, Halphen C, Boska MD, Narayana PA. Diffusion tensor metrics, T2 relaxation, and volumetry of the naturally aging human caudate nuclei in healthy young and middle-aged adults: possible implications for the neurobiology of human brain aging and disease. Magn Reson Med. 2008; 59(1):7–13. [PubMed: 18050345]

Hayasaka S, Phan KL, Liberzon I, Worsley KJ, Nichols TE. Nonstationary cluster-size inference with random field and permutation methods. Neuroimage. 2004; 22(2):676–87. [PubMed: 15193596]

Herndon JG, Tigges J, Klumpp s.A. Anderson DC. Brain weight does not decrease with age in adult rhesus monkeys. Neurobio Aging. 1998; 19(3):267–72.

Karalis KP, Giannogonas P, Kodela E, Koutmani Y, Zoumakis M, Teli T. Mechanisms of obesity and related pathology: linking immune responses to metabolic stress. FEBS J. 2009; 276(20):5747–54. [PubMed: 19754872]

Katsaros VK, Glocker FX, Hemmer B, Schumacher M. MRI of spinal cord and brain lesions in subacute combined degeneration. Neuroradiology. 1998; 40(11):716–9. [PubMed: 9860120]

Kemnitz JW, Weindruch R, Roecker EB, Crawford K, Kaufman PL, Ershler WB. Dietary restriction of adult male rhesus monkeys: design, methodology, and preliminary findings from the first year of study. J Gerontol. 1993; 48(1):B17–26. [PubMed: 8418134]

Kennedy KM, Raz N. Aging white matter and cognition: differential effects of regional variations in diffusion properties on memory, executive functions, and speed. Neuropsychologia. 2009; 47(3): 916–27. [PubMed: 19166865]

Kim WK, Pae YS. Involvement of N-methyl-d-aspartate receptor and free radical in homocysteine-mediated toxicity on rat cerebellar granule cells in culture. Neurosci Lett. 1996; 216(2):117–20. [PubMed: 8904797]

Kondo M, Shibata R, Miura R, Shimano M, Kondo K, Li P, Ohashi T, Kihara S, Maeda N, Walsh K, Ouchi N, Murohara T. Caloric restriction stimulates revascularization in response to ischemia via adiponectin-mediated activation of endothelial nitric-oxide synthase. J Biol Chem. 2009; 284(3): 1718–24. [PubMed: 18990685]

Kwa VI, Zaal LH, Verbeeten B Jr. Stam J, Amsterdam Vascular Medicine Group. Disequilibrium in patients with atherosclerosis: relevance of pontine ischemic rarefaction. Neurology. 1998; 51(2): 570–3. [PubMed: 9710037]

Lentz SR, Sobey CG, Piegors DJ, Bhopatkar M, Faraci FM, Malinow MR, Heistad DD. Vascular dysfunction in monkeys with diet-induced hyperhomocyset(e)inemia. J Clin Invest. 1996; 98:24–9. [PubMed: 8690798]

Lentz SR, Piegors DJ, Malinow MR, Heistad DD. Supplementation of atherogenic diet with B vitamins does not prevent atherosclerosis or vascular dysfunction in monkeys. Circulation. 2001; 103:1006–1011. [PubMed: 11181477]

Lenzi D, Conte A, Mainero C, Frasca V, Fubelli F, Totaro P, Caramia F, Inghilleri M, Pozzilli C, Pantano P. Effect of corpus callosum damage on ipsilateral motor activation in patients with multiple sclerosis: a functional and anatomical study. Hum Brain Mapp. 2007; 28(7):636–44. [PubMed: 17080438]

Longstreth WT Jr. Katz R, Olson J, Bernick C, Carr JJ, Malinow MR, Hess DL, Cushman M, Schwartz SM. Plasma total homocysteine levels and cranial magnetic resonance imaging findings in elderly persons: the Cardiovascular Health Study. Arch Neurol. 2004; 61(1):67–72. [PubMed: 14732622]

Mangas A, Covenas R, Geffard K, Geffard M, Marcos P, Insausti R, Dabdie MP. Folic acid in the monkey brain: an immunocytochemical study. Neurosci Lett. 2004; 362(2):258–61. [PubMed: 15158027]

Marlatt MW, Lucassen PJ, Perry G, Smith MA, Zhu X. Alzheimer's disease: cerebrovascular dysfunction, oxidative stress, and advanced clinical therapies. J Alzheimers Dis. 2008; 15(2):199–210. [PubMed: 18953109]

McCully KS. The biomedical significance of homocysteine. J Scient Exploration. 2001; 15(1):5–20.

McLaren DG, Kosmatka KJ, Oakes TR, Kroenke CD, Kohama SG, Matochik JA, Ingram DK, Johnson SC. A population-average MRI-based atlas collection of the rhesus macaque. Neuroimage. 2009; 45(1):52–9. [PubMed: 19059346]

McLaren DG, Kosmatka KJ, Kastman EK, Bendlin BB, Johnson SC. Rhesus macaque brain morphometry: A methodological comparison of voxel-wise approaches. Methods. 2010; 50(3): 157–65. 2010 Mar. [PubMed: 19883763]

Morra JH, Tu Z, Apostolova LG, Green AE, Avedissian C, Madsen SK, Parikshak N, Hua X, Toga AW, Jack CR Jr. Schuff N, Weiner MW, Thompson PM. Automated 3D mapping of hippocampal atrophy and its clinical correlates in 400 subjects with Alzheimer's disease, mild cognitive impairment, and elderly controls. Hum Brain Mapp. 2009 Epub ahead of print.

Nurk E, Refsum H, Tell GS, Engedal K, Vollset SE, Ueland PM, Nygaard HA, Smith AD. Plasma total homocysteine and memory in the elderly: the Hordaland Homocysteine Study. Ann Neurol. 2005; 58(6):847–57. [PubMed: 16254972]

Oldreive CE, Doherty GH. Neurotoxic effects of homocysteine on cerebellar Purkinje neurons in vitro. Neurosci Lett. 2007; 413(1):52–7. [PubMed: 17157438]

Paxinos, G.; Huang, X-F.; Petrides, M.; Toga, A. The Rhesus Monkey Brain in Stereotaxic Coordinates. 2nd ed.. Academic Press; San Diego: 2009.

Pearce JM. Central pontine myelinolysis. Eur Neurol. 2009; 61(1):59–62. [PubMed: 19033724]

Preston AM, Bercovitch FB, Jimenez BD, Rodriguez Orengo JF, Morales WD, Rodriguez CA, Lebron MR, Rivera CE. Plasma homocysteine concentrations in a population of rhesus monkeys (Macaca mulatta): reference ranges and accompanying plasma concentrations of folate and vitamin B12. Contemp Topics in Lab Anim Sci. 2002; 41(1):28–30.

Pullicino P, Ostrow P, Miller L, Snyder W, Munschauer F. Pontine ischemic rarefaction. Ann Neurol. 1995; 37(4):460–6. [PubMed: 7717682]

Ramsey JJ, Colman RJ, Binkley NC, Christensen JD, Gresl TA, Kemnitz JW, Weindruch R. Dietary restriction and aging in rhesus monkeys: the University of Wisconsin study. Exp Gerontol. 2000; 35(9-10):1131–49. [PubMed: 11113597]

Roth GS, Mattison JA, Ottinger MA, Chachich ME, Lane MA, Ingram DK. Aging in rhesus monkeys: relevance to human health interventions. Science. 2004; 305(5689):1423–6. [PubMed: 15353793]

Sachdev P. Homocysteine, cerebrovascular disease and brain atrophy. J Neurol Sci. 2004; 226(1-2): 25–9. [PubMed: 15537514]

Sachdev PS. Homocysteine and brain atrophy. Prog Neuropsychopharmacol Biol Psychiatry. 2005; 29(7):1152–61. [PubMed: 16102882]

Saleem KS, Pauls JM, Augath M, Trinath T, Prause BA, Hashikawa T, Logothetis NK. Magnetic resonance imaging of neuronal connections in the macaque monkey. Neuron. 2002; 34(5):685–700. [PubMed: 12062017]

Schmahmann, J.; Pandya, D. Fiber pathways of the brain. Oxford UP; New York: 2006.

Seshadri S, Wolf PA, Beiser AS, Selhub J, Au R, Jacques PF, Yoshita M, Rosenberg IH, D'Agostino RB, DeCarli C. Association of plasma total homocysteine levels with subclinical brain injury: cerebral volumes, white matter hyperintensity, and silent brain infarcts at volumetric magnetic resonance imaging in the Framingham Offspring Study. Arch Neurol. 2008; 65(5):642–9. [PubMed: 18474741]

Shirpoor A, Salami S, Khadem-Ansari MH, Minassian S, Yegiazarian M. Protective Effect of Vitamin E Against Ethanol-Induced Hyperhomocysteinemia, DNA Damage, and Atrophy in the Developing Male Rat Brain. Alcohol Clin Exp Res. 2009 Epub ahead of print.

Smolin LA, Benevenga NJ. The use of cyst(e)ine in the removal of protein-bound homocysteine. Am J Clin Nutr. 1984; 39(5):730–7. [PubMed: 6711475]

Song SK, Sun SW, Ramsbottom MJ, Chang C, Russell J, Cross AH. Dysmyelination revealed through MRI as increased radial (but unchanged axial) diffusion of water. Neuroimage. 2002; 17(3):1429–36. [PubMed: 12414282]

Sowell ER, Peterson BS, Thompson PM, Welcome SE, Henkenius AL, Toga AW. Mapping cortical change across the human life span. Nat Neurosci. 2003; 6(3):309–15. [PubMed: 12548289]

Thomas AJ, Davis S, Ferrier IN, Kalaria RN, O'Brien JT. Elevation of cell adhesion molecule immunoreactivity in the anterior cingulate cortex in bipolar disorder. Biol Psychiatry. 2004; 55(6): 652–5. [PubMed: 15013836]

Ungvari Z, Parrado-Fernandez C, Csiszar A, de Cabo R. Mechanisms underlying caloric restriction and lifespan regulation: implications for vascular aging. Circ Res. 2008; 102(5):519–28. [PubMed: 18340017]

Vatanavicharn N, Pressman BD, Wilcox WR. Reversible leukoencephalopathy with acute neurological deterioration and permanent residua in classical homocystinuria: A case report. J Inherit Metab Dis. 2008 Epub ahead of print.

Vermeer SE, van Dijk EJ, Koudstaal PJ, Oudkerk M, Hofman A, Clarke R, Breteler MM. Homocysteine, silent brain infarcts, and white matter lesions: The Rotterdam Scan Study. Ann Neurol. 2002; 51(3):285–9. [PubMed: 11891822]

Wilhelm J, Frieling H, von Ahsen N, Hillemacher T, Kornhuber J, Bleich S. Apolipoprotein E polymorphism, homocysteine serum levels and hippocampal volume in patients with alcoholism: an investigation of a gene-environment interaction. Pharmacogenomics J. 2008; 8(2):117–21. [PubMed: 17420762]

Willette AA, Lubach GR, Coe CL. Environmental context differentially affects behavioral, leukocyte, cortisol, and interleukin-6 responses to low doses of endotoxin in the rhesus monkey. Brain Behav Immun. 2007; 21(6):807–15. [PubMed: 17336039]

Wisco JJ, Killany RJ, Guttmann CRG, Warfield SK, Moss MB, Rosene DL. An MRI study of age-related white and gray matter volume changes in the rhesus monkey. Neurobio Aging. 2008; 29(10):1563–75.

Wong A, Mok V, Fan YH, Lam WW, Liang KS, Wong KS. Hyperhomocysteinemia is associated with volumetric white matter change in patients with small vessel disease. J Neurol. 2006; 253(4):441–7. [PubMed: 16267639]

Xiao S, Hansen DK, Horsley ET, Tang YS, Khan RA, Stabler SP, Jayaram HN, Antony AC. Maternal folate deficiency results in selective upregulation of folate receptors and heterogeneous nuclear ribonucleoprotein-E1 associated with multiple subtle aberrations in fetal tissues. Birth Defects Res A Clin Mol Teratol. 2005; 73(1):6–28. [PubMed: 15641086]

Zylberstein DE, Lissner L, Bjorkelund C, Mehlig K, Thelle DS, Gustafson D, Ostling S, Waern M, Guo X, Skoog I. Midlife homocysteine and late-life dementia in women. A prospective population study. Neurobiol Aging. 2009 Epub ahead of print.

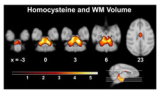

Figure 1.
Axial slices depicting areas of lower white matter volume associated with higher serum Hcy levels in neurological space. The two main clusters encompassed basis pontis and middle cerebellar peduncle, which contains ponto-cerebellar fibers, and the body of the corpus callosum. The ‘warm’ color bar represents the magnitude of t-values.

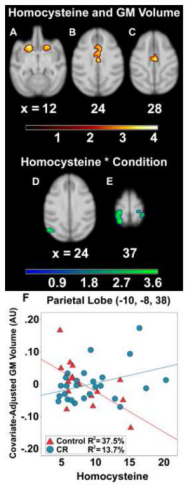

Figure 2.

Main effect association of Hcy and Hcy*Condition interaction on regional gray matter volume in neurological space. Hcy was correlated with lower gray matter in: bilateral striatum (**A**); anterior cingulate cortex (**B**); and mid cingulate cortex (**C**). The interaction tested where CR monkeys, per μmol/L unit increase in Hcy, showed a reduced relationship between Hcy and lower gray matter relative to controls. Regions implicated in the interaction after statistical correction included visual cortices (**D**), parietal areas (**E**), and right hippocampus (not shown). A representative voxel in left parietal lobe illustrates the interaction (**F**). The 'warm' and 'green-blue' color bars represent t-values for the association and interaction analyses respectively. gray matter volume is depicted in arbitrary units (AU).

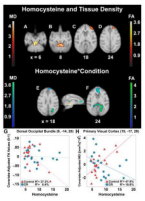

Figure 3.

Correlation of Hcy concentrations and the Hcy*Condition interaction with fractional anisotropy and mean diffusivity values in neurological space. The ‘orange’ and yellow’ t-statistic color maps respectively represent areas where greater Hcy levels were associated with higher mean diffusivity and lower fractional anisotropy. Hcy was correlated with lower fractional anisotropy in middle cerebellar peduncle (**A**). Higher mean diffusivity was seen in anterior cerebellum and the same peduncle (**B**); orbital and ventral prefrontal cortices (**C**); dorsal prefrontal cortex gray matter and corticocortical fibers (**D**). For the interaction, the ‘green’ (fractional anisotropy) and ‘blue’ (mean diffusivity) color maps show where CR monkeys had a mitigated correlation between Hcy and tissue density per μmol/L unit increase relative to controls. Regions implicated included the visual cortices (**E**) and medial prefrontal cortex within the cingulate sulcus (**F**). Representative voxels in dorsal occipital bundle (**G**) and primary visual cortex (**H**) illustrate the interaction for changes in fractional anisotropy and mean diffusivity.

Table 1

Negative association between white matter volume and homocysteine.

Region	Coordinates (x, y, z)	Peakt-value	Cluster Size (voxels)
R Dorsal Pons	6, 2, 3	5.21	27674
L Dorsal Pons	−5, 8, 4	4.98	
L&R Medial Anterior Lobe of Cerebellum	−2, −1, 7	4.59	
Body of CC	1, 15, 22	3.64	1809

L = left hemisphere; R = right hemisphere. CC = Corpus Callosum. Result maps had a voxel and cluster threshold of $p < .005$ (uncorrected) and $p < .05$ (corrected) respectively.

Table 2

Negative association of gray matter volume, homocysteine, and mediation by dietary condition.

Region	Coordinates (x, y, z)	Peakt-value	Cluster size (voxels)
Homocysteine associations			
L&R Anterior Cingulate Cortex	2, 13, 25	4.12	2323
L&R Anterior Cingulate Cortex	0, 26, 22	3.55	
L Caudoputamen	−10, 28, 12	3.79	2021
L Agranular Insula	−16, 25, 7	2.76	
R Putamen	10, 28, 12	3.47	1372
L Dorsal Premotor Cortex	−8, 26, 32	3.30	2260
L Dorsal Premotor Cortex	−8, 40, 32	3.11	
Homocysteine*Condition			
L Somatosensory areas 1 and 2	−10, −8, 38	3.74	3325
L visual area 7a	−11, 0, 38	3.53	
R Somatosensory area 5	7, 0, 40	3.60	2004
R Hippocampus	17, 16, 0	3.58	247
R visual area 7a	14, −2, 36	3.01	
L Extrastriate Cortex	−20, −12, 22	3.44	3964
L Primary Visual Cortex	−16, −18, 28	3.20	
L Extrastriate Cortex (LS)	−13, −9, 23	2.90	

L = Left hemisphere; R = Right hemisphere. LS = Lunate Sulcus. The interaction tested where CR monkeys showed more gray matter relative to controls per unit increase in Hcy, suggesting an ameliorative effect. Voxel and cluster thresholds were $p < .005$ (uncorrected) and $p < .05$ (corrected) respectively. The hippocampal result survived a cluster correction derived from an *a priori* defined anatomical ROI.

Table 3

Negative association of homocysteine, fractional anisotropy, and mediation by dietary condition.

Fiber tract	Coordinates (x, y, z)	Peakt-value	Cluster size (voxels)
Homocysteine associations			
R Pontocerebellar fibers	0,6,7	3.68	1448
Homocysteine*Condition			
R Occipito-splenial Fibers	10, −12, 20	4.23	5784
Splenium of CC	10, −2, 18	4.14	
Splenium of CC	0, 2, 17	3.73	

L = Left hemisphere; R = Right hemisphere. CC = Corp us Callosum. The interaction tested where CR monkeys showed more fractional anisotropy relative to controls per unit increase in Hcy, suggesting a protective effect. The voxel and cluster thresholds were $p < .005$ (uncorrected) and $p < .05$ (corrected) respectively.

Table 4

Positive association of homocysteine, mean diffusivity, and mediation by dietary condition.

Region	Coordinates (x, y, z)	Peakt-value	Cluster size (voxels)
Homocysteine associations			
L Medial Anterior Lobe of Cerebellum	−6, −5, 8	4.49	2243
R Medial Anterior Lobe of Cerebellum	6, −4, 8	4.20	
R Dorsal Prefrontal Cortex	9, 40, 24	3.93	1363
R Ventral Prefrontal Cortex	17, 38, 18	3.53	
Homocysteine*Condition			
R Anterior Cingulate Cortex	2, 36, 18	3.85	4398
L Medial Prefrontal Cortex	−2, 44, 14	3.11	
R Dorsal Prefrontal Cortex	3, 44, 22	2.96	
R Primary Visual Cortex	19, −17, 29	3.83	1322
R Primary Visual Cortex	14, −22, 27	3.60	

L = Left hemisphere; R = Right hemisphere. The interaction tested where CR monkeys showed less mean diffusivity relative to controls per unit increase in Hcy, suggesting a protective effect. The voxel and cluster thresholds were $p < .005$ (uncorrected) and $p < .05$ (corrected) respectively.